Perspective

Supramolecular chemistry of dendrimers with functional cores

François Diederich* and Béatrice Felber

Laboratorium für Organische Chemie, Eidgenössische Technische Hochschule-Hönggerberg, HCI, CH-8093 Zürich, Switzerland

Dendritic microenvironments are analogous to local environments created within protein superstructures. Correspondingly, properties of functional cores such as molecular recognition and catalytic activity are profoundly influenced by the surrounding dendritic branches.

A higher-generation dendrimer of globular shape comprises three distinct topological regions, namely surface, dendritic branching, and central core (1–3). The branched shell produces a unique microenvironment around the encapsulated core (4), similar to the local environments generated at active sites within protein superstructures. In our research, we became interested in exploring how the branching repeats, and the micropolarity they create, influence the molecular recognition (5–7) and catalytic properties of buried dendritic cores (8, 9). Therefore, we synthesized two families of dendritic receptors featuring cyclophane-type (*dendrophanes*) or cleft-type (*dendroclefts*) recognition sites (10, 11) as cores as well as a series of dendritically encapsulated metalloporphyrins (12–16). The model character of these compounds for biological receptors and globular heme proteins was nicely revealed in subsequent studies that are summarized in this perspective article. They clearly demonstrate that dendritic superstructures are highly effective in modulating chemical and physical properties of the encapsulated core (17–20).

Dendritic Cyclophanes (Dendrophanes)

The two series of first- to third-generation (G-1 to G-3) dendrophanes **1–3** and **4–6** (Fig. 1) with poly(ether amide) branching and 12, 36, and 108 terminal carboxyl groups, respectively, were prepared as the first water-soluble dendrimers with a defined active recognition site at the central core (21–23). Whereas series **1–3** features a central cyclophane core with a binding cavity complementary in size to benzene and naphthalene guests, the second series **4–6** was designed to complex large steroidal substrates. The third-generation dendrimers **3** and **6** have molecular weights (M_r) around 18,000. The compounds were prepared by divergent and semiconvergent synthesis and shown by matrix-assisted laser-desorption ionization–time-of-flight (MALDI-TOF) mass spectrometry and ^{13}C-NMR spectroscopy to be of high purity and monodispersity. Attempts to prepare a monodisperse fourth-generation dendrophane with an M_r above 56,000 failed, and only a polydisperse mixture of incompletely coupled products was isolated after purification by gel permeation chromatography (GPC) (22).

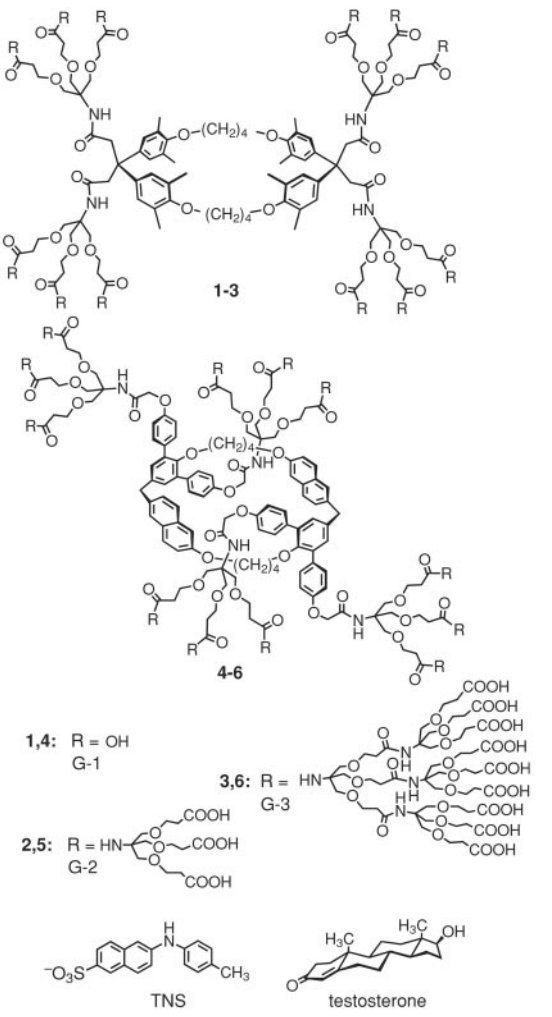

Fig. 1. Two series of dendrophanes of first (G-1), second (G-2), and third (G-3) generation for apolar complexation with fast binding kinetics in aqueous solution. Compounds **1–3** contain a cyclophane core with a cavity complementary to benzene and naphthalene derivatives; compounds **4–6** possess an expanded cyclophane cavity for the inclusion of steroids.

The binding properties of the generation 1–3 dendrophanes, in comparison with those of the core cyclophanes, were investigated in basic aqueous buffers by using ^{1}H-NMR and fluorescence binding titrations. The following results were obtained.

*To whom reprint requests should be addressed. E-mail: diederich@org.chem.ethz.ch.

www.pnas.org/cgi/doi/10.1073/pnas.052568099

(*i*) The preorganized cyclophane recognition sites (24) at the center of the dendrophanes remain open and effective at all dendritic generation levels. Hydrophobic collapse of the dendritic branches with inhibitory occupation of the cyclophane cavity-binding site apparently is not very effective. The stability of the inclusion complexes formed at the cyclophane core is nearly independent from the dendritic generation level. Thus, the formation free enthalpy of complexes formed by the fluorescence probe 6-(*p*-toluidino)naphthalene-2-sulfonate (TNS) and dendrophanes **1–3** changed from $\Delta G^\circ = -5.5$ (G-1) to -5.3 (G-2), and to -5.1 kcal mol^{-1} (G-3; 300 K, fluorescence titrations). Similarly, the formation free enthalpy for the complexes between testosterone and the dendrophanes **4–6** was nearly independent on generation [$\Delta G^\circ = -3.9$ to 4.1 kcal mol^{-1}; 298 K, ^{1}H-NMR titrations in borate-buffered D_2O (pD 10.5)/CD_3OD 1:1]. In all complexes, the substrates are exclusively located in the central cyclophane cavities as revealed by large and specific complexation-induced changes in chemical shift of the cyclophane and guest resonances measured during ^{1}H-NMR titrations. Nonspecific incorporation into fluctuating voids in the dendritic shell is negligible.

(*ii*) With increasing dendritic generation, the micropolarity around the core cyclophane is significantly reduced. Fluorescence titrations with TNS in aqueous phosphate buffer (pH 8.0) showed that the micropolarity at the core of G-3 dendrophane **3** is comparable to that of ethanol.

(*iii*) Host-guest exchange kinetics are fast ($k_{decompl} > 10^2$–10^3 s^{-1}) even at the G-3 level. This result from ^{1}H-NMR titrations and fluorescence relaxation measurements with fluorescent steroidal substrates is in sharp contrast to the findings by Meijer and coworkers (25), who observed substrate encapsulation with half-lifetimes of hours and days in their poly(propylene imine) dendrimers. This difference originates from differences in core size: The Meijer dendrimers feature a tight, densely packed superstructure diverging from a small initiator core. In contrast, the four dendritic wedges in the dendrophanes are attached to large, nanometer-sized cyclophane cores, which produces apertures through which substrates can rapidly enter or leave the binding cavity. Furthermore, the Meijer systems possess strongly H-bonding and sterically encumbering surface groups that generate tight substrate encapsulation at the interior, whereas the carboxylates at the dendrophane surfaces will not densely pack for electrostatic reasons.

The reduced micropolarity at the central cyclophane core and the fast host-guest exchange kinetics made water-soluble dendrophanes attractive targets for further development into catalytic dendrophanes, mimics of globular enzymes. Therefore, we prepared dendrimers (similar to **2**) with a thiazolium ion-substituted cyclophane core as functional mimics of the thiamine-pyrophosphate-dependent enzyme pyruvate oxidase (26) and investigated their activity as catalysts in the oxidation of naphthalene-2-carbaldehyde to methyl naphthalene-2-carboxylate. This reaction is known to benefit in its rate from a reduced environmental polarity around the catalytic thiazolium ion (27). However, studies in basic aqueous methanol revealed only a weak catalytic activity of the dendritic thiazolio-cyclophanes, despite the demonstrated favorable micropolarity at the cyclophane active site. The observed low catalytic activity in the interior of the macromolecules is best explained by steric hindrance of reaction transition states by the dendritic branches. Apparently, the dendritic enzyme models suffer from the lack of secondary structure within the branches. The ordered protein shell around an enzyme active site not only ensures a correct positioning of the catalytic residues at that site and modulates its polarity, but also keeps this site open and free of steric hindrance for the reaction of the correct substrate. Thus, one of the future challenges in the design of dendrimers with interior catalytic sites is the implementation of defined secondary structural motifs within the branching.

Dendrophanes have also been successfully applied to dendritic self-assembly (28, 29). Large multinanometer-sized assemblies with M_r exceeding 14,000 were obtained in aqueous methanol (pH 8.7) by threading two dendrophanes **5** onto an about 5.5-nm-long molecular rod, in which two testosterone termini are attached by rigid oligo(phenylacetylene) spacers to a central phenyl ring bearing quaternary ammonium side chains (30). The formation of these aggregates, in which the dendrophanes preferentially encapsulate the steroidal termini, is driven by a combination of apolar forces, hydrophobic desolvation, and ion pairing, and depends strongly on the correct length of the rigid oligo(phenylacetylene) spacers. Even much larger structurally defined supramolecular aggregates with M_r approaching 100,000 can be envisaged, in which four G-3 dendrophanes **6** are threaded onto four steroids attached to suitably sized spacers diverging from a tetrahedral focal point.

Dendritic Cleft-Type Receptors (Dendroclefts)

Optically active spiro[9*H*-bifluorenes] bearing 2,6-bis(carbonylamino)pyridine moieties in the 2,2′-positions form stoichiometric 1:1 complexes with monosaccharides via H-bonding in noncompetitive solvents (31). We became interested in incorporating such clefts as cores into dendrimers with branches that lack H-bond donor sites (32) to see how the dendritic environment would influence sugar binding affinity and selectivity (33). The formation of stable 1:1 complexes (association constants K_a between 100 and 600 M^{-1}, $CDCl_3$, 298 K) between dendroclefts (−)-**7** (G-0), (−)-**8** (G-1), and (−)-**9** (G-2) with octyl glucosides **10–12** (Fig. 2) was shown in ^{1}H-NMR and CD titrations as well as by Job plot analyses. The major host-guest bonding interactions in these complexes are N–H···O H-bonds between the amide NH groups at the core and the O-atoms of the monosaccharides as well as N···H–O H-bonds between the pyridine N-atoms and the HO groups of the guests. The stereoselectivity of the recognition processes is profoundly altered by the degree of dendritic branching. Whereas the enantioselectivity drops sharply with increasing dendritic generation [from (−)-**7** to (−)-**9**], the diastereoselectivity increases markedly in the same direction. The analysis of complexation-induced changes in ^{1}H-NMR chemical shift suggest that, with increasing dendritic generation, the N–H···O host-guest H-bonding becomes weakened and these interactions are increasingly replaced by O···H–O H-bonds between the ether O-atoms of the dendritic branches and the sugar OH groups. The CD spectra of the receptors also respond to guest complexation in an unambiguous and stereoselective manner. The measured guest-selective chiroptical effects clearly illustrate the potential of dendritic receptors to function as sensors for biologically important substrates. One of the advantages of dendritic sugar-sensing is the easy recyclability of the receptors: As a consequence of their higher molecular masses, simple filtration over a GPC plug allows full recovery of the dendroclefts whereas the smaller monosaccharide guests are being retained on the plug.

Dendritic Iron Porphyrins with Tethered Axial Ligands As Model Compounds for Cytochromes

Dendritically encapsulated metalloporphyrins have attracted wide interest as models for globular heme proteins, and the dendritic generation-dependence of properties of the metalloporphyrin core has been intensively investigated (12–16). Examples are hemoglobin- and myoglobin-like gas binding ability (34–36), heme monooxygenase activity (14, 37), electron acceptor capacity in light-harvesting antenna systems (38), and shell-modulated redox potentials as found in cytochromes (39–41). We discuss here the model character of dendritic iron porphyrins with tethered axial ligands for cytochromes (42, 43). The most intriguing characteristic of the cytochrome family of electron transfer proteins is the very broad range of redox potentials featured by the Fe^{III}/Fe^{II} couple at the electroactive heme core (44). The heme microenvironment, created by the surrounding protein shell, has been identified as a major factor

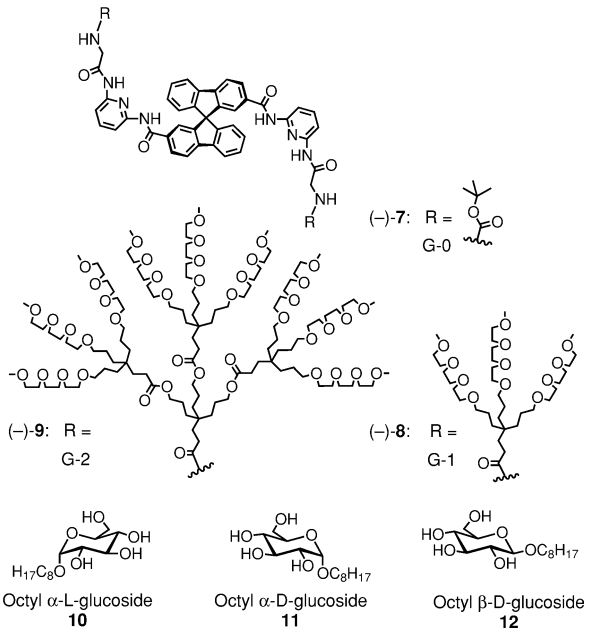

Fig. 2. Dendroclefts (−)-**7** (G-0), (−)-**8** (G-1), and (−)-**9** (G-2) stereoselectively form 1:1 complexes with monosaccharides **10–12** in $CHCl_3$.

influencing the redox potentials that are substantially anodically shifted (by 300–400 mV) compared with simple heme model systems lacking the peptide coverage. We had prepared a series of dendritic iron porphyrins as model compounds for cytochromes (39–41), in which the protein shell around the buried electroactive core was mimicked by the dendritic superstructure. However, the nature of the axial ligation to the iron center, which is known to have a very strong influence on the redox properties (45), was not controlled in these earlier systems. Therefore, the observed potential shifts caused by the dendritic shell could not be quantified independently from axial ligation effects and no general conclusions concerning the effects of the dendritic superstructure could be drawn. We subsequently prepared the three novel dendrimers **13** (G-0), **14** (G-1), and **15** (G-2) (Fig. 3) featuring axial ligation by two tethered imidazoles. This ligation pattern is thermodynamically stable as well as kinetically inert toward coordinating solvents and is found in the cytochrome-b_5 family of electron transfer proteins (46). All three compounds are six-coordinate low-spin Fe^{III} complexes, and the potential of their Fe^{III}/Fe^{II} couple was investigated by cyclic voltammetry in CH_2Cl_2 and MeCN as well as by optical redox titrations in H_2O. In all three solvents, large anodic potential shifts were seen (up to 380 mV) with increasing dendritic generation level (Table 1).

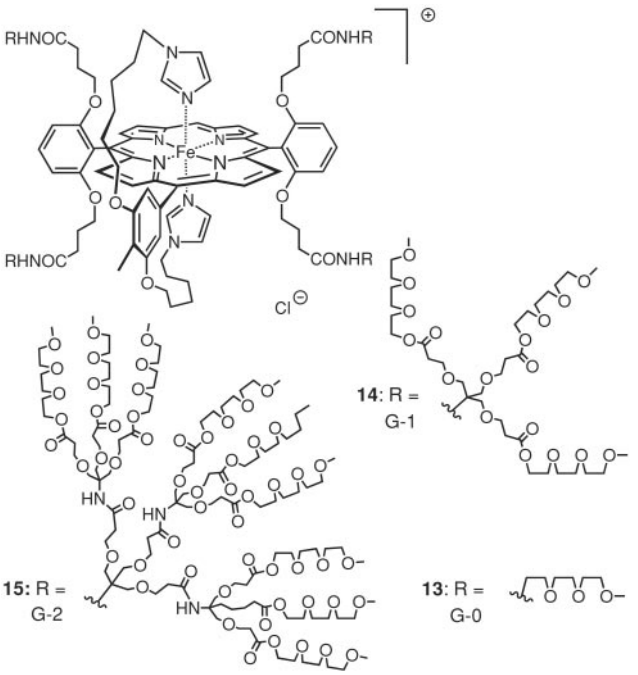

Fig. 3. Dendritic model compounds **13–15** for cytochrome-b_5.

The following noticeable results were obtained (Fig. 4). (*i*) In all solvents investigated, the redox potential of the Fe^{III}/Fe^{II} couple became more positive with increasing dendritic generation. Remarkably, the potential of the G-2 complex **15** [M_r = 11,719; comparable in mass and size to typical single heme cytochromes such as *Bonita* cytochrome-*c* (M_r = 11,384) or bovine cytochrome-b_5 (M_r = 15,198)] is, within experimental error, identical in all three solvents of extremely different polarity (Fig. 4). This finding clearly demonstrates that the dendritic branching creates a unique local microenvironment around the isolated electroactive core. The dendritic shell fully mimics the protecting peptide shell that modulates the redox potential of the Fe^{III}/Fe^{II} couple in a similar way in cytochromes.

(*ii*) In the two organic solvents, the largest shift to more positive potential occurs after changing from the G-0 to the G-1 complex (Fig. 4). Clearly, the special microenvironment at the dendritic core is already largely created by the G-1 branching in these solvents.

(*iii*) In sharp contrast, the redox potential in H_2O does not vary much after passing from the G-0 to the G-1 complex. Solvation effects are much more pronounced in water, and the relatively open dendritic branches in **14** do not impede access of bulk solvent to the central core for the stabilization of the Fe^{III} state.

Table 1. Redox potentials (V vs. SCE) of the Fe^{III}/Fe^{II} couple in 13–15 in different solvents

	E (Fe^{III}/Fe^{II})		
Porphyrin	CH_2Cl_2*	MeCN*	H_2O
13 (G-0)	−0.21	−0.24	−0.29†
14 (G-1)	+0.08	−0.01	−0.25†
15 (G-2)	+0.10	+0.09	+0.09‡

*Values from cyclic voltammetry (CV) approximated as $E_{1/2} = (E_{pa} - E_{pc})/2$; supporting electrolyte 0.1 M Bu_4NPF_6; glassy carbon working electrode, Ag/AgCl reference electrode, Pt wire counter electrode; T = 298 K; scan rate = 0.1 V·s^{-1}.
†Values from equilibrium measurements with $[Fe(ox)_3]^{4-/3-}$ as reference compound; T = 298 K.
‡Values from equilibrium measurements with $[Fe(CN)_6]^{4-/3-}$ as reference compound; T = 298 K.

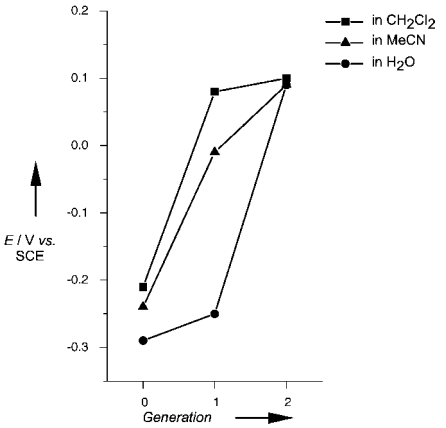

Fig. 4. Plot of the redox potentials (V vs. SCE) of the Fe^{III}/Fe^{II} couples of **13–15** in different solvents as a function of the dendritic generation.

However, in the G-2 complex **15**, the dendritic superstructure is sufficiently dense to prevent the contact between heme and external bulk solvent, thereby creating the same, unique core microenvironment as in organic solvents.

(*iv*) The shift to more positive potentials with increasing dendritic generation in H_2O can be readily explained by the increased shielding of the electroactive core from the polar bulk solvent. The reduced solvation of the charged Fe^{III} porphyrin core leads to an energetic destabilization of this state with respect to the charge-neutral Fe^{II} species, which is much less affected by the weaker solvation. In contrast, the analogous trend observed in the organic solvents is much harder to rationalize. As these two solvents are less polar than the dendritic shell, one would rather expect a stabilization of the polar oxidized state with increasing encapsulation and exclusion of bulk solvent, leading to a lowering of the redox potential. This is, however, clearly not the case. Obviously there are other effects besides controlling solvent access and solvent-mediated charge stabilization, which the dendritic shell exerts on the shielded electrophore at its core. These probably are related to its detailed chemical nature, conformational dynamics, and hydrodynamic volume and are not well understood at present.

Conclusions

Dendrons and dendritic shells of multinanometer dimensions are powerful new tools to modulate recognition, catalysis, and redox processes at sites buried at the core of dendrimers. By creating efficient new microenvironments in their interior, dendrimers provide fascinating mimics of globular protein shells. However, dendrimers at present have the disadvantage—as compared with proteins—that their three-dimensional structure and conformational dynamics are not well understood. One of the future challenges in the design of dendrimers with functional interior sites is the implementation of defined secondary-structural motifs within the branches. This design could greatly improve catalytic processes at dendrimer cores by minimizing steric hindrance of the reaction transition states by the branching. Such defined secondary structural motifs could also enhance the crystallinity of the usually oily macromolecules and enable their (highly desirable) structural characterization by x-ray crystallography. Clearly, with better structural characterization and more defined secondary and tertiary structure, fundamental and technological research opportunities offered by dendrimers as well as their model character for globular proteins could be greatly enhanced.

This research was supported by the Eidgenössische Technische Hochschule research council, the Office of Naval Research, and by Hoffmann–La Roche.

1. Newkome, G. R., Moorefield, C. N. & Vögtle, F. (1996) *Dendritic Molecules: Concepts, Syntheses, Perspectives* (VCH, Weinheim, Germany).
2. Vögtle, F., ed. (1998) *Dendrimers, Top. Curr. Chem.* (Springer, Berlin), Vol. 197.
3. Vögtle, F., ed. (2000) *Dendrimers II, Top. Curr. Chem.* (Springer, Berlin), Vol. 210.
4. Hawker, C. J., Wooley, K. L. & Fréchet, J. M. J. (1993) *J. Am. Chem. Soc.* **115,** 4375–4378.
5. Smith, D. K. & Diederich, F. (2000) in *Dendrimers II, Top. Curr. Chem.*, Vögtle, F., ed. (Springer, Berlin), pp. 183–227.
6. Baars, M. W. P. L. & Meijer, E. W. (2000) in *Dendrimers II, Top. Curr. Chem.*, Vögtle, F., ed. (Springer, Berlin), pp. 131–182.
7. Zeng, F. & Zimmerman, S. C. (1997) *Chem. Rev.* **97,** 1681–1712.
8. Newkome, G. R., He, E. & Moorefield, C. N. (1999) *Chem. Rev.* **99,** 1689–1746.
9. Oosterom, G. E., Reek, J. N. H., Kamer, P. C. J. & van Leeuwen, P. W. N. M. (2001) *Angew. Chem. Int. Ed. Engl.* **40,** 1828–1849.
10. Pugh, V. J., Hu, Q.-S., Zuo, X., Lewis, F. D. & Pu, L. (2001) *J. Org. Chem.* **66,** 6136–6140.
11. Zimmerman, S. C., Wang, Y., Barathi, P. & Moore, J. S. (1998) *J. Am. Chem. Soc.* **120,** 2172–2173.
12. Hecht, S., Ihre, H. & Fréchet, J. M. J. (1999) *J. Am. Chem. Soc.* **121,** 9239–9240.
13. Vinogradov, S. A. & Wilson, D. F. (2000) *Chem. Eur. J.* **6,** 2456–2461.
14. Bhyrappa, P., Young, J. K., Moore, J. S. & Suslick, K. S. (1996) *J. Am. Chem. Soc.* **118,** 5708–5711.
15. Kimura, M., Shiba, T., Yamazaki, M., Hanabusa, K., Shirai, H. & Kobayashi, N. (2001) *J. Am. Chem. Soc.* **123,** 5636–5642.
16. Enomoto, M. & Aida, T. (1999) *J. Synth. Org. Chem. Jpn.* **57,** 924–934.
17. Gorman, C. B. & Smith, J. C. (2001) *Acc. Chem. Res.* **34,** 60–71.
18. Cardona, C. M., Mendoza, S. & Kaifer, A. E. (2000) *Chem. Soc. Rev.* **29,** 37–42.
19. Burn, P. L., Beavington, R., Frampton, M. J., Pillow, J. N. G., Halim, M., Lupton, J. M. & Samuel, I. D. W. (2001) *Mater. Sci. Eng.* **B85,** 190–194.
20. Smith, D. K. & Müller, L. (1999) *Chem. Commun.*, 1915–1916.
21. Mattei, S., Seiler, P., Diederich, F. & Gramlich, V. (1995) *Helv. Chim. Acta* **78,** 1904–1912.
22. Wallimann, P., Seiler, P. & Diederich, F. (1996) *Helv. Chim. Acta* **79,** 779–788.
23. Mattei, S., Wallimann, P., Kenda, B., Amrein, W. & Diederich, F. (1997) *Helv. Chim. Acta* **80,** 2391–2417.
24. Wallimann, P., Mattei, S., Seiler, P. & Diederich, F. (1997) *Helv. Chim. Acta* **80,** 2368–2390.
25. Jansen, J. F. G. A., de Brabander-van den Berg, E. M. M. & Meijer, E. W. (1994) *Science* **266,** 1226–1229.
26. Habicher, T., Diederich, F. & Gramlich, V. (1999) *Helv. Chim. Acta* **82,** 1066–1095.
27. Mattei, P. & Diederich, F. (1997) *Helv. Chim. Acta* **80,** 1555–1588.
28. Zimmerman, S. C., Zeng, F., Reichert, D. E. C. & Kolotuchin, S. V. (1996) *Science* **271,** 1095–1098.
29. Tomioka, N., Takasu, D., Takahashi, T. & Aida, T. (1998) *Angew. Chem. Int. Ed. Engl.* **37,** 1531–1534.
30. Kenda, B. & Diederich, F. (1998) *Angew. Chem. Int. Ed. Engl.* **37,** 3154–3158.
31. Cuntze, J., Owens, L., Alcazar, V., Seiler, P. & Diederich, F. (1995) *Helv. Chim. Acta* **78,** 367–390.
32. Smith, D. K., Diederich, F. & Zingg, A. (1999) in *Supramolecular Science: Where It Is and Where It Is Going*, eds. Ungaro, R. & Dalcanale, E. (Kluwer, Dordrecht, The Netherlands), pp. 261–272.
33. Bähr, A., Felber, B., Schneider, K. & Diederich, F. (2000) *Helv. Chim. Acta* **83,** 1346–1376.
34. Jiang, D.-L., Aida, T. (1996) *Chem. Commun.*, 1523–1524.
35. Collman, J. P., Fu, L., Zingg, A. & Diederich, F. (1997) *Chem. Commun.*, 193–194.
36. Zingg, A., Felber, B., Gramlich, V., Fu, L. Collman, J. P. & Diederich, F. (2002) *Helv. Chim. Acta* **85,** in press.
37. Weyermann, P. & Diederich, F. (2002) *Helv. Chim. Acta* **85,** in press.
38. Choi, M.-S., Aida, T., Yamazaki, T. & Yamazyki, I. (2001) *Angew. Chem. Int. Ed. Engl.* **40,** 3194–3198.
39. Dandliker, P. J., Diederich, F., Gross, M., Knobler, C. B., Louati, A. & Sanford, E. M. (1994) *Angew. Chem. Int. Ed. Engl.* **33,** 1739–1742.
40. Dandliker, P. J., Diederich, F., Gisselbrecht, J.-P., Louati, A. & Gross, M. (1995) *Angew. Chem. Int. Ed. Engl.* **34,** 2725–2728.
41. Dandliker, P. J., Diederich, F., Zingg, A., Gisselbrecht, J.-P., Gross, M., Louati, A. & Sanford, E. (1997) *Helv. Chim. Acta* **80,** 1773–1801.
42. Weyermann, P., Gisselbrecht, J.-P., Boudon, C., Diederich, F. & Gross, M. (1999) *Angew. Chem. Int. Ed. Engl.* **38,** 3215–3219.
43. Weyermann, P., Diederich, F., Gisselbrecht, J.-P., Boudon, C. & Gross, M. (2002) *Helv. Chim. Acta* **85,** in press.
44. Moore, G. R. & Pettigrew, G. W. (1990) *Cytochromes-c: Evolutionary, Structural and Physicochemical Aspects* (Springer, Berlin).
45. Raphael, A. L. & Gray, H. B. (1991) *J. Am. Chem. Soc.* **113,** 1038–1040.
46. Mathews, F. S., Levine, M. & Argos, P. (1971) *Nat. New Biol.* **233,** 15–16.